International Journal of Astrobiology 14 (4): 547–553 (2015)
doi:10.1017/S1473550415000014

Hexagonal plate-like magnetite nanocrystals produced in komatiite–H_2O–CO_2 reaction system at 450°C

Xi-Luo Hao and Yi-Liang Li

Department of Earth Sciences, The University of Hong Kong, Pokfulam Road, Hong Kong, China
e-mail: yiliang@hku.hk

Abstract: Batch experiments of komatiite–H_2O–CO_2 system with temperatures from 200 to 450°C were performed to simulate the interactions between the newly formed ultramafic crust and the proto-atmosphere on Earth before the formation of its earliest ocean. Particularly, magnetite nanocrystals were observed in the experiment carried out at 450°C that are characterized by their hexagonal platelet-like morphology and porous structure. Exactly the same set of lattice fringes on the two opposite sides of one pore suggests post-crystallization erosion. The results demonstrate that magnetite could be produced by the direct interactions between the ultramafic rocky crust and the atmosphere before the formation of the ocean on the Hadean Earth. These magnetite nanoparticles could serve as a catalyst in the synthesis of simple organic molecules during the organochemical evolution towards life.

Received 18 May 2014, accepted 20 December 2014, first published online 22 April 2015

Key words: magnetite, prebiotic evolution, water–rock interaction

Introduction

Geological records indicate that life has been present on Earth for at least 3.5 Gyr, and life probably began as early as 3.8 billion years ago (Ga) (Nisbet 1987; Nisbet & Fowler 1996). Right after the Moon-forming impact that occurred at about 4.5 Ga (Valley *et al.* 2014), the surface of Earth turned into a magma ocean that was unsuitable for life to start. However, there were critical steps for the early Earth to evolve from a hell of fire to a habitable planet in the Hadean eon. Unfortunately, because of the extensive geological reworking, there is almost no petrologic record for this piece of history (e.g. Valley *et al.* 2014). Current knowledge on Earth's Hadean environment suggests that the proto-atmosphere formed a few million years after the Moon-forming impact, was composed of a few hundred bars of water steam, 100–200 bars of CO_2 and small amount of CO, H_2, etc. (Condie 1980; Walker 1985; Liu 2004; Zahnle 2006; Zahnle *et al.* 2007; Sleep 2010). The continuous cooling of the Earth's surface had led to the condensation of the atmospheric water steam and subsequently the formation of the earliest ocean (Martin *et al.* 2006) before 4.4 Ga (Wilde *et al.* 2001; Valley *et al.* 2014). The early interactions between lithosphere, atmosphere and ocean of the Earth not only changed the physicochemical condition of the Earth's surface, but also initiated the prebiotic chemistry towards life. To understand these early planetary processes, most studies have focused on the Earth with a hydrosphere because life was emerged from aqueous environment (Russell *et al.* 1989, 1994; Fruth-Green *et al.* 2004; Holm *et al.* 2006; Schulte *et al.* 2006; Martin & Russell 2007). Serpentinization in the hydrothermal environment is then suggested to be one important process due to its highly chemically active mineral assemblages and catalysed synthesis of simple organic molecules (Russell *et al.* 2010). However, before the formation of the earliest ocean, the supercritical H_2O–CO_2 proto-atmosphere might have reacted with the newly solidified crust and these direct interactions should be different from the water–rock interactions after the formation of the ocean. This direct atmosphere–rock interaction could have significant impact on the chemistries of the early atmosphere and the crust.

Sepentinization can produce Fe- and Ni-bearing sulphides, oxides and native metal alloys that could play critical roles in catalysing the reduction of primordial CO_2 to organic molecules, and further the formation of biopolymers (Yoshida *et al.* 1993; Horita & Berndt 1999; Chen & Bahnemann 2000; Fu *et al.* 2007; Pizzarello 2012; McCollom & Seewald 2013). As an important secondary mineral, magnetite in such processes has been experimentally investigated by many previous studies (Berndt *et al.* 1996; Seyfried *et al.* 2007; Marcaillou *et al.* 2011). These studies mainly paid attention to the detection of magnetite to constrain its formation conditions during serpentinization, but overlooked its crystal habits, which is critical in catalysing the organosynthesis. Because of the low productivity, Seyfried *et al.* (2007) only detected magnetite in the run product using vibrating sample magnetometer. Marcaillou *et al.* (2011) identified magnetite using X-ray diffraction (XRD) in the product of hydrothermal alteration of peridotite. Magnetite crystals were only directly observed by Normand *et al.* (2002) and McCollom & Seewald (2013) that showed octahedral shapes with the size of a few to tens

Table 1. *Summary of the initial experimental conditions for the CO_2–H_2O–komatiite batch experiments*

Experiment no.	Initial materials			Temperature (°C)	Pressure (bar)	Run duration (days)
	Komatiite (mg)	$Ag_2C_2O_4$/equivalent CO_2 (mg)	H_2O (mg)			
K-450P	35.2	26.7/7.7	68.8	450	500	14
K-400P	32.1	23.1/6.7	61.7	400	500	14
K-350P	26.4	26.9/7.8	51.3	350	500	14
K-300P	27.6	25.2/7.3	50.1	300	500	14
K-250P	23.8	26.4/7.6	52.4	250	500	14
K-200P	24.1	24.7/7.1	50.9	200	500	14
K-200PL	25.5	23.9/6.9	53.8	200	500	30

micrometres. These limited observations are insufficient for the understanding of its catalytic property and geochemical fates.

In the present study, we conducted batch experiments to simulate the interaction between the crust and proto-atmosphere at the earliest evolution stage of the Earth. Followed by our experiments, we examined the formation of secondary minerals especially magnetite to gain some new insights into the direct interactions between atmosphere and lithosphere and their influence on the mineral evolution and the prebiotic chemical evolution on the early Earth.

Materials and methods

Distilled deionized (DD) water was used as the starting liquid phase to avoid the participation of alkaline in reactions occurred in the batch experiments. Since CO_2 cannot be directly added into the Au capsule, $Ag_2C_2O_4$ was used as the source of CO_2 in the batch experiments. Fresh $Ag_2C_2O_4$ was prepared by the aqueous reaction between $H_2C_2O_4$ and excess $AgNO_3$ (equation 1). The precipitated $Ag_2C_2O_4$ was centrifuged and washed by DD water for at least three times to completely remove $AgNO_3$. Once the autoclave is heated, $Ag_2C_2O_4$ breaks down to pure Ag and CO_2 (equation 2).

$$2AgNO_3 + H_2C_2O_4 \cdot 6H_2O \rightarrow Ag_2C_2O_4 + 2HNO_3 + 6H_2O, \quad (1)$$

$$Ag_2C_2O_4 \rightarrow 2Ag + 2CO_2. \quad (2)$$

As the reduced chemical species (for example, CO, CH_4 and H_2) in the proto-atmosphere only constituted very small fractions of Earth's earliest atmosphere (Condie 1980; Walker 1985; Liu 2004; Zahnle 2006; Zahnle *et al.* 2007; Sleep 2010), they would not play substantial roles in the interaction between the proto-atmosphere and the ultramafic crust. Therefore, the H_2O–CO_2 system was used to represent the proto-atmosphere. Fresh komatiite from Zimbabwe with typical spinifex texture and characterized by high Mg content, high $Fe^{2+}/\Sigma Fe$ and relatively high content of Ni and Cr (Nisbet *et al.* 1987; Berry *et al.* 2008) was used to represent the earliest crustal ultramafic rocks interacting with the proto-atmosphere. The value of $Fe^{2+}/\Sigma Fe$ in komatiite was measured by the ^{57}Fe Mössbauer spectroscopy with a 25mCi ^{57}Co/Pb source at the University of Hong Kong. The finely ground komatiite was prepared as absorbent with relative thicknesses of ~5 mg Fe cm^{-2}. Spectra were collected at room temperature in transmission mode with a constant acceleration mode. The velocity scale was calibrated relative to 25 μm α-Fe at room temperature. Lorentzian doublets were used for fitting the areas of sub-spectra.

The experiments were carried out at Hydrothermal Laboratory at Guangzhou Institute of Geochemistry, Chinese Academy of Sciences. All materials were weighted and loaded into a flexible Au capsule. Then the Au capsule was put in Ar atmosphere and sealed by a welding machine to protect the materials from being oxidized. The water–rock ratio was adjusted to approximately 2 : 1 and $Ag_2C_2O_4$ was restricted to a suitable amount to avoid the explosion of the sealed Au capsule. The sealed Au capsule was then put into a steel alloy autoclave. The pressure inside the autoclave was monitored by a barometer and temperature was controlled by a digital temperature controller. Batch Experiments were carried out by heating the autoclave to a constant temperature under 500 bar pressure for at least 2 weeks. The temperature varied from 200 to 450°C with an increment of 50°C. At the end of experiment, the autoclave was quenched to room temperature in a few seconds with ice water. Blank experiment loaded with pure $Ag_2C_2O_4$ and water was also conducted to examine the compositions of the gas phase from the decomposing of $Ag_2C_2O_4$. The experimental conditions were summarized in Table 1.

The morphology of solid products after experiments was observed by a Hitachi S-4800 field-emission scanning electron microscope (SEM) at the University of Hong Kong. The accelerating voltage was set to 3–5 kV so as to take SEM images with fine surface structures. Energy-dispersive X-ray spectroscopic (EDS) measurements were also carried out at 20 kV to measure the chemical compositions. However, the EDS analyses could only provide limited information because the secondary minerals were always adhered to the host rock that contributed strong background signals. A FEI Tecnai G2 20 S-TWIN scanning transmission electron microscope (STEM) was used to characterize the crystallographic structures of secondary minerals. Specimens were loaded on copper grids with carbon-coated formvar and examined in the normal STEM mode to obtain bright images using an accelerating voltage of 200 kV. Detailed structure information of minerals was obtained by selected area electron diffraction (SAED) patterns and high-resolution transmission electron microscopy (HRTEM) micrographs.

The volatile components in the Au capsule were analysed by an Agilent 6890 N gas chromatograph (GC) connected with a gas-collection system. Firstly, the sealed Au capsule was cleaned and put into the gas-collection system. After the

https://doi.org/10.1017/S1473550415000014 Published online by Cambridge University Press

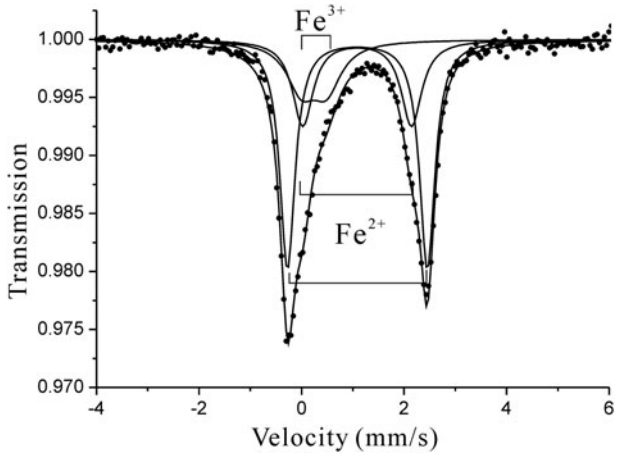

Fig. 1. Mössbauer spectrum of komatiite powder.

whole system was evacuated, the Au capsule was pierced and the sealed volatile components would fulfil the gas-collection system. The valve between the gas-collection system and 6890 N GC was then opened to allow gases to get into the GC. The organic and inorganic gas components were analysed in an automatically controlled procedure.

Results and discussion

Mössbauer spectroscopy and $Fe^{2+}/\Sigma Fe$ of komatiite

Since komatiite used in this study is consisted of multiple types of minerals/materials, the site distribution of Fe^{2+} and Fe^{3+} can hardly be assigned accurately. Therefore, the spectrum was fitted with two Fe^{2+} doublets and one Fe^{3+} doublet (Fig. 1). Doublet with quadrupole splitting (QS)=0.49 mm s^{-1} and isomer shift (IS)=0.24 mm s^{-1} was assigned to paramagnetic Fe^{3+} in silicates; while the doublet with QS=2.73 mm s^{-1}, and IS=1.09 mm s^{-1} and doublet with QS=2.12 mm s^{-1} and IS=1.09 mm s^{-1} were both assigned to paramagnetic Fe^{2+} in silicates. The $Fe^{2+}/\Sigma Fe$ ratio of komatiite was 0.80 based on the fitting of the spectra.

Nucleation of magnetite

The SEM observation showed abundant clay minerals and carbonates stack on the initial komatiite in the run-products (Fig. 2). Clay minerals can be found in all experiments with different temperatures, whereas carbonates can only be found in experiments with temperature below 400°C. The EDS analyses showed that the formed phyllosilicates containing less amount of Fe than those in olivine and glass matrix of the original komatiite. This result indicated that a portion of the Fe released from the glass matrix and the fayalite component of olivine was sequestered by other secondary minerals. As described by many previous studies, serpentinization of ultramafic rocks is always coupled with the production of H_2 (Barnes *et al.* 1972; Moody 1976; Frost 1985; Berndt *et al.* 1996; Marcaillou *et al.* 2011) owing to the oxidation of Fe(II) on the lattice of minerals to Fe(III) by water. H_2 was detected in all experiments with variable concentrations (from tens to hundreds ppm). The oxidation of Fe(II) activated from silicates would probably lead to the nucleation of magnetite and it has been reported in several previous serpentization experiments (Berndt *et al.* 1996; Seyfried *et al.* 2007; Marcaillou *et al.* 2011). However, magnetite was not observed in our experiments carried out between 200 and 400°C. The only experiment in which magnetite was observed was carried out at 450°C. This temperature is higher than that of previous serpentinization experiments (mostly between 200 and 300°C) in which magnetite was reported (Berndt *et al.* 1996; Seyfried *et al.* 2007; Marcaillou *et al.* 2011). One possible reason for the lack of magnetite in our lower temperature experiments (conducted between 200 and 400°C) is the relatively short run duration compared with previous experiments (up to several thousand hours). As shown by Marcaillou *et al.* (2011), magnetite can only be detected in the latest stages of hydrothermal alteration of peridotite at 300°C/300 bar after 70 days. The thermodynamic modelling (Klein *et al.* 2009) have showed that both the partitioning and the oxidation state of iron are sensitive to temperature and water/rock ratio, while the formation of magnetite depends on the availability of an external source of silica at higher temperature. With low temperature and low water/rock ratio, Fe^{3+} is allowed to partition into silicates that may also account for the lack of magnetite under these conditions. For example, Seyfried *et al.* (2007) carried out the serpentinization experiment at 200°C and 500 bar; likewise, their results showed the production of H_2 but little magnetite. Another possible reason for the difference in the magnetite formation conditions between our experiments and previous studies is the activity of CO_2. The fugacity–fugacity diagram of the Fe–C–O–H system shows that siderite is the most stable phase under relatively reduced condition with high CO_2 fugacity under reduced condition and pH values >5 (Fig. 3). In our experiments, the high CO_2 fugacity may result in the incorporation of Fe into carbonates while the prevention of magnetite crystallization. The EDS analysis of the carbonates formed in our experiments also confirmed the incorporation of iron into the carbonates (Fig. 2).

The crystallography of magnetite

Magnetite produced at 450°C was characterized by TEM (Figs 4 and 5). Unlike the conventional octahedral crystal habits that have been commonly observed in previous experiments (McCollom & Seewald 2013), magnetite crystals produced in this study were hexagonal plates of a few hundred nanometres (Fig. 5). The EDS analyses showed that the platelike magnetite nanocrystals also contained small amount of Ni and Cr (~7 wt% Ni and 1 wt% Cr). SAED analysis of the crystals (Fig. 4(b)) yields Miller indices (*hkl*) of (220), (311), (440) and (511) that confirmed the electron diffraction pattern of magnetite (Table 2). The TEM images showed porous structures on magnetite crystals (Figs 4 and 5). The pores on the thin magnetite crystals revealed that the crystals were thin hexagonal nanocrystals rather than the projection of octahedral magnetite crystals. HRTEM images showing exactly the same set of lattice fringes at the opposite sides of one pore on the magnetite crystals (Fig. 4(d)) suggested that the porous

https://doi.org/10.1017/S1473550415000014 Published online by Cambridge University Press

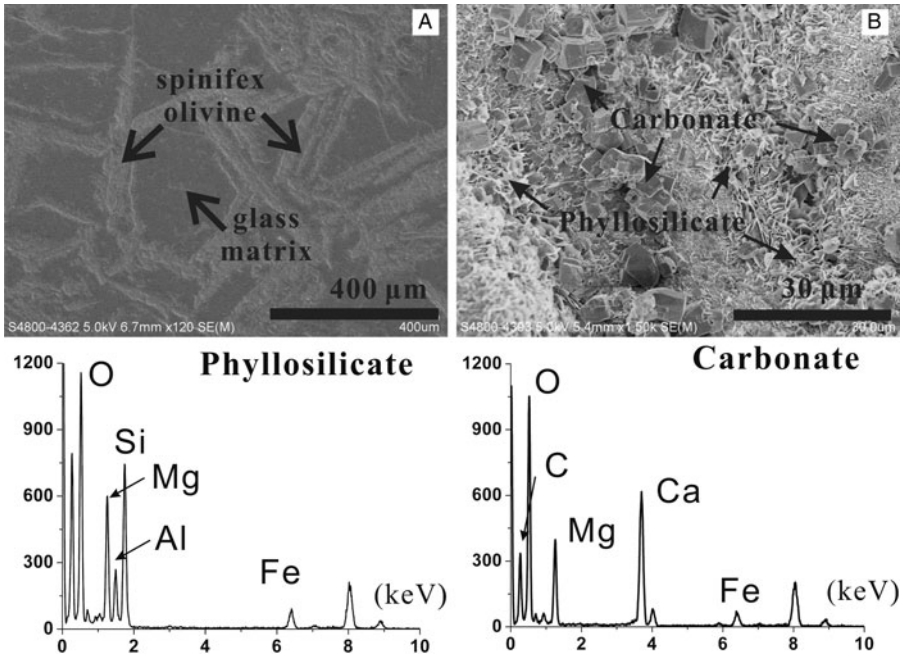

Fig. 2. SEM image of komatiite before (A) and after (B) the experiment. The observed typical secondary minerals are phyllosilicate and carbonate (300°C).

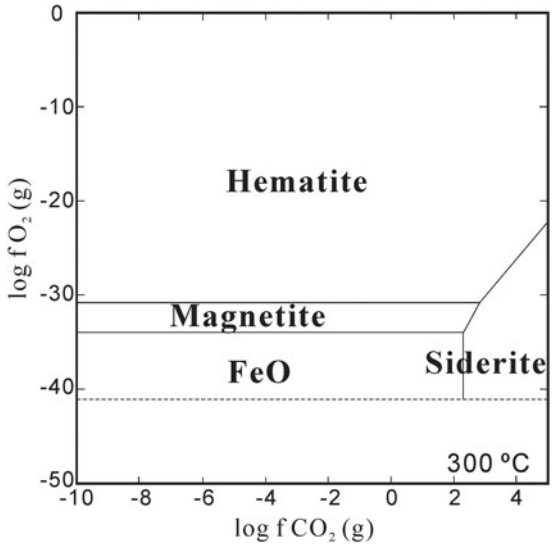

Fig. 3. The influence of CO_2 and O_2 fugacity to the stabilities of iron species in P–T condition similar to our experiments. The DIAGRAM was calculated with Geochemists Workbench (Bethke 1996) with the Lawrence Livermore National Laboratory database.

structure was produced after the crystallization of magnetite. The measured spacing of the crystallographic planes was 0.29 nm (Fig. 4(d)), equals to the *d*-space of (220) planes of magnetite crystals (PDF800389), implying that these magnetite nanocrystals grew along the [110] direction.

Various experimental studies have showed that magnetite can act as catalyst in abiotic synthesis of small organic molecules such as hydrocarbons, amino acids and acetic acid (Chen & Bahnemann 2000; Fu *et al.* 2007; Pizzarello 2012). All these reactions are heterogeneous catalyses in which the total surface area of catalyst has a critical effect on the reaction rate because it determines the availability of catalytic sites (Swathi & Sebastian 2008). Taken Fischer–Tropsch synthesis of methane as an example, the catalytic reaction happens on the surface of catalyst (magnetite) in high-H_2 environments in which iron carbides are formed (Satterfield *et al.* 1986a, b; Lee *et al.* 1990) that can act as reaction intermediates. Compared with magnetite observed in the serpentinization experiments, smaller size and the porous structure of magnetite platelets observed in this study make them have lager specific surface area that favours the catalysis of abiotic synthesis.

In our experiment, nickel and chromium were the other two transition metals found incorporated in magnetite, implying its potential in catalysing multiple types of simple organics. These two metals have been demonstrated be important in abiotic synthesis of hydrocarbons. Foustoukos & Seyfried (2004) suggest that chromite ($FeCr_2O_4$) was an efficient catalyst for Fischer-Tropsch type (FTT) synthesis of longer chain hydrocarbons. Horita & Berndt (1999) reported the excellent catalytic capability of awaruite (a Ni–Fe alloy) in the conversion from CO_2 to CH_4. As in the original komatiite, Ni and Cr are minor components with the concentrations of several thousand ppm. Although Ni–Fe-alloys, Ni/Cr oxides and sulphides were not observed in our experiments due probably to the short run duration and lack of sulphur compound in the komatiite, geological observation and thermodynamic calculation (Klein & Bach 2009; McCollom & Seewald 2013) consistently demonstrate that these minerals could form under hydrothermal conditions. Together with magnetite, they constitute the common accessory minerals in serpentiniation in the hydrothermal systems (McCollom & Seewald 2013).

https://doi.org/10.1017/S1473550415000014 Published online by Cambridge University Press

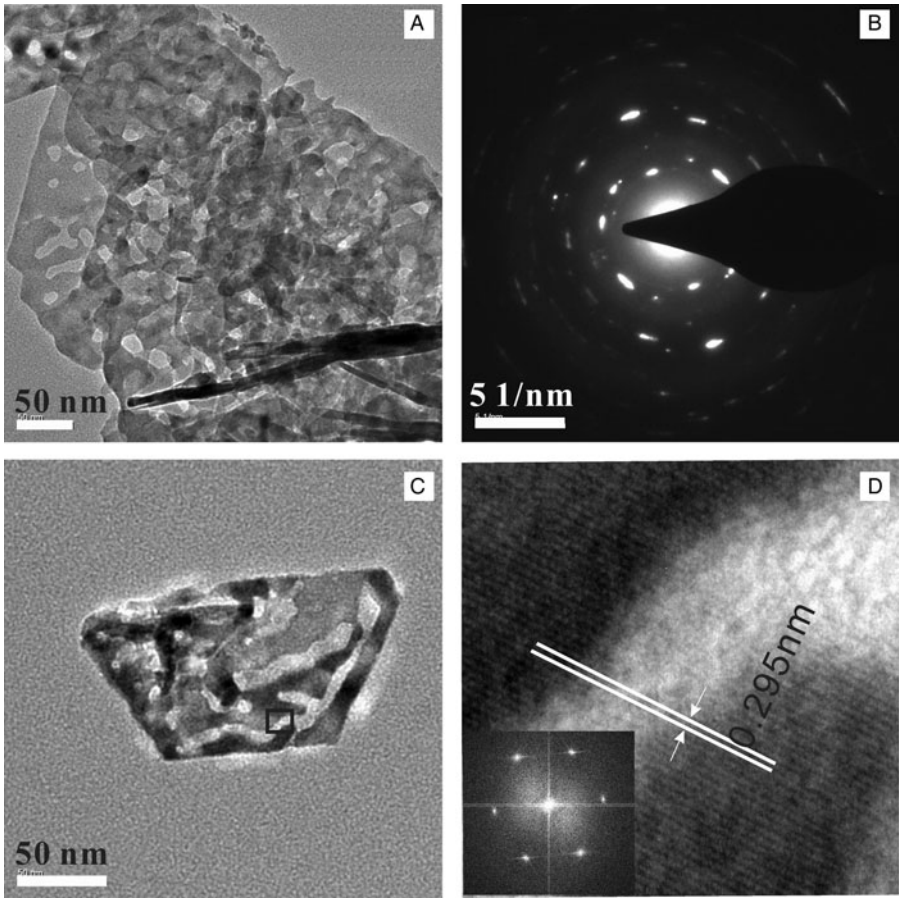

Fig. 4. TEM characterization of Fe-oxide found in higher temperature experiments (450°C). Panel (B) shows the SAED pattern of this mineral from (A), which indicates that the secondary mineral is magnetite. (D) The HRTEM image of selected part of (C) showing the same interplanar spacings at both sides of one pore.

Implication for the organosynthesis of the prebiotic evolution on the early Earth

It has been proposed previously that alkaline hydrothermal vent is a favourite site for the origin and early evolution of life because the physicochemical conditions favour the prebiotic chemical processes (Russell *et al.* 1989, 1994, 2010; Fruth-Green *et al.* 2004; Sleep *et al.* 2004, 2011; Holm *et al.* 2006; Schulte *et al.* 2006; Martin & Russell 2007). Experimental simulations and examinations of geological samples (Berndt *et al.* 1996; McCollom *et al.* 2001; McCollom & Seewald 2003a, b, 2004, 2007; Seewald *et al.* 2006; Seyfried *et al.* 2007) have showed that methane, short hydrocarbons and minor formate, methanol and trace acetate (these may also be the by-products of microbial activity) can be produced by serpentinization in the hydrothermal systems. In addition, laboratory experiments (Horita & Berndt 1999; Chen & Bahnemann 2000; Foustoukos & Seyfried 2004) have showed that many of these organic compounds can be produced with Fe-, Cr- and Ni-bearing oxides, sulphides as catalysts.

According to the results of our batch experiments, magnetite can be produced quickly at a temperature of 450°C. As the physicochemical conditions we chose for the experiments are similar to the Hadean Earth with H_2O steam and high CO_2 in the atmosphere, thus the formed magnetite could accumulate before the formation of the earliest ocean by 4.4 Ga (Wilde *et al.* 2001; Valley *et al.* 2014). Being so, reactions associated with the abiotic synthesis of acetate or other simple organic compounds from CO_2, as catalysed by Fe and Ni oxide/sulphide minerals, might have already happened at an earlier time before the emergence of the earliest ocean. Meanwhile, the abiotic synthesis of organic molecules would occur widespread since the global occurrence of the reaction between the ultramafic crust and the CO_2–H_2O dominant atmosphere. Although the surface temperature was too high for the organic molecules to be preserved long enough, they may gradually accumulate along with the catalytic secondary minerals on the early Earth and led to the origin of life after the cooling of the Earth's surface (Holm & Andersson 1998; Martin & Russell 2007).

Conclusion remarks

Experiments simulating the interaction between the rock crust and atmosphere on the Hadean Earth were performed using komatiite, H_2O and CO_2 from 200 to 450°C to investigate the production of secondary minerals. The results showed the

https://doi.org/10.1017/S1473550415000014 Published online by Cambridge University Press

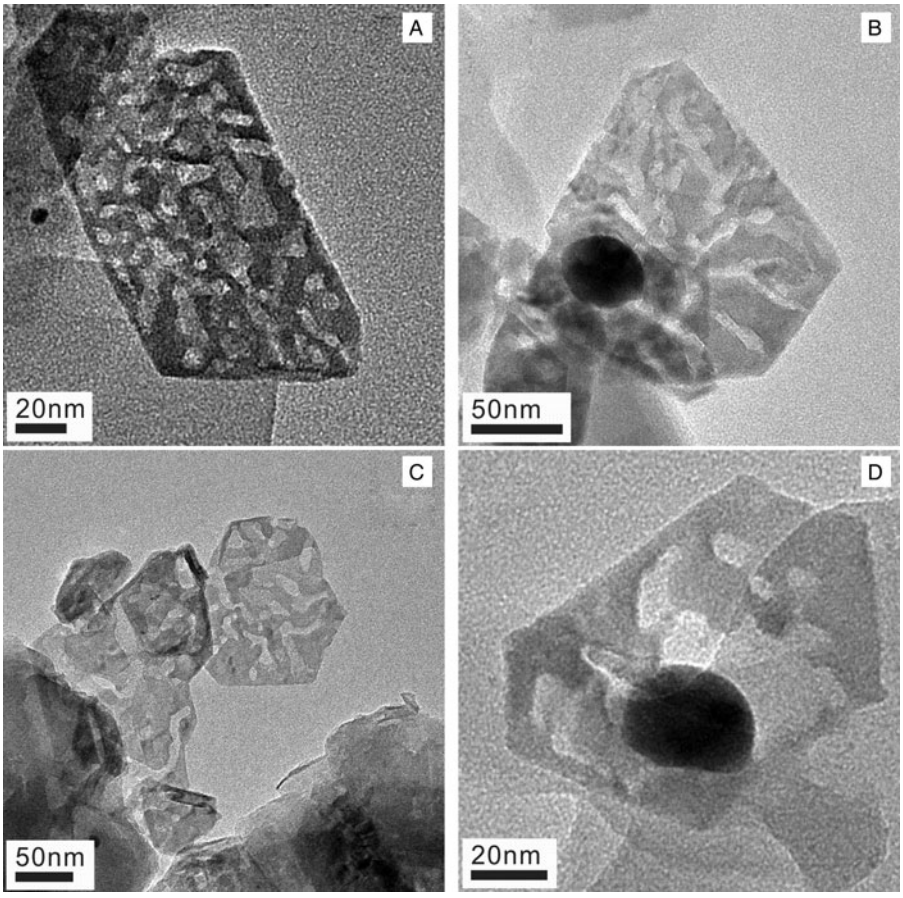

Fig. 5. TEM image of plate-like magnetite nanocrystals. (A), (B), (C) and (D) show the hexagonal crystal shape of magnetite nanocrystals.

Table 2. *Electron diffraction data for magnetite crystals*

Magnetite nanoplates (Å)	Magnetite (Å)[a]	(*hkl*)
2.961	2.9687	(220)
2.522	2.5317	(311)
2.101	2.0992	(400)
1.634	1.6159	(511)
1.478	1.4843	(440)

[a]PDF: 86–1326.

secondary minerals are mainly phyllosilicates and carbonates. The formation of magnetite was only confirmed in experiment carried out at 450°C. Particularly, magnetite crystals observed in this study is hexagonal plates of a few hundred nanometres. This is the first report and characterization of plate-like magnetite nanocrystals in water–rock experiments. The porous structures on magnetite crystals are very likely the result of post-crystallization erosion. The detection of magnetite in our experiments suggests a general formation and accumulation of magnetite nanoparticle on Earth' surface before the formation of its earliest ocean. With these magnetite nanoparticles and the other catalytic minerals, the prebiotic chemical evolution could start early and extensively than previously thought.

Acknowledgements

We thank Professor Weidong Sun and Dr. Xing Ding for their advices on our experiments and the support from the Hydrothermal Laboratory at Guangzhou Institute of Geochemistry, Chinese Academy of Sciences. This study was financially supported by Research Grants Council of Hong Kong (HKU703911P).

References

Barnes, I., Sheppard, R.A., Gude, A.J., Rapp, J.B. & Oneil, J.R. (1972). Metamorphic assemblages and direction of flow of metamorphic fluids in 4 instances of serpentinization. *Contrib. Miner. Petrol* **35**(3), 263–276.

Berndt, M.E., Allen, D.E. & Seyfried, W.E. (1996). Reduction of CO_2 during serpentinization of olivine at 300°C and 500 bar. *Geology* **24**(4), 351–354.

Berry, A.J., Danyushevsky, L.V., O'Neill, H.SC., Newville, M. & Sutton, S.R. (2008) Oxidation state of iron in komatiitic melt inclusions indicates hot Archaean mantle. *Nature* **455**, 960–963.

Bethke, C.M. (1996). *Geochemical Reaction Modeling*. Oxford University Press, New York.

Chen, Q.W. & Bahnemann, D.W. (2000). Reduction of carbon dioxide by magnetite: implications for the primordial synthesis of organic molecules. *J. Am. Chem. Soc.* **122**(5), 970–971.

Condie, K.C. (1980). Origin and early development of the Earth's crust. *Precambrian Res.* **11**(3–4), 183–197.

https://doi.org/10.1017/S1473550415000014 Published online by Cambridge University Press

Foustoukos, D.I. & Seyfried, W.E. (2004). Hydrocarbons in hydrothermal vent fluids: the role of chromium-bearing catalysts. *Science* **304**, 1002–1005.

Frost, B.R. (1985). On the stability of sulfides, oxides, and native metals in serpentinite. *J Petrol* **26**(1), 31–63.

Fruth-Green, G.L., Connolly, J.A.D., Plas, A., Kelley, D.S. & Grobety, B. (2004). Serpentinization of oceanic peridotites: implications for geochemical cycles and biological activity. *Geophys. Monogr. Ser.* **144**, 119–136.

Fu, Q., Lollar, B.S., Horita, J., Lacrampe-Couloume, G. & Seyfried, W.E. (2007). Abiotic formation of hydrocarbons under hydrothermal conditions: constraints from chemical and isotope data. *Geochim. Cosmochim. Acta* **71**(8), 1982–1998.

Holm, N.G. & Andersson, E.M. (1998). Hydrothermal systems. In *The Molecular Origins of Life, Assembling Pieces of the Puzzle*, ed. Brack, A., pp. 86–99. Cambridge University Press, Cambridge.

Holm, N.G., Dumont, M., Ivarsson, M. & Konn, C. (2006). Alkaline fluid circulation in ultramafic rocks and formation of nucleotide constituents: a hypothesis. *Geochem. Trans.* **7**, 7. doi: 10.1186/1467-4866-7-7.

Horita, J. & Berndt, M.E. (1999). Abiogenic methane formation and isotopic fractionation under hydrothermal conditions. *Science* **285**(5430), 1055–1057.

Klein, F. & Bach, W. (2009). Fe–Ni–Co–O–S phase relations in peridotite–seawater interactions. *J. Petrol* **50**(1), 37–59.

Klein, F., Bach, W., Jons, N., McCollom, T., Moskowitz, B. & Berquo, T. (2009). Iron partitioning and hydrogen generation during serpentinization of abyssal peridotites from 15 degrees N on the Mid-Atlantic Ridge. *Geochim. Cosmochim. Acta* **73**(22), 6868–6893.

Lee, M.D., Lee, J.F. & Chang, C.S. (1990). Catalytic behavior and phase-composition change of iron catalyst in hydrogenation of carbon-dioxide. *J. Chem. Eng. Jpn.* **23**(2), 130–136.

Liu, L.G. (2004). The inception of the oceans and CO_2-atmosphere in the early history of the Earth. *Earth Planet. Sci. Lett.* **227**(3–4), 179–184.

Marcaillou, C., Munoz, M., Vidal, O., Parra, T. & Harfouche, M. (2011). Mineralogical evidence for H_2 degassing during serpentinization at 300° C/300 bar. *Earth Planet. Sci. Lett.* **303**(3–4), 281–290.

Martin, H., Albarede, F., Claeys, P., Gargaud, M., Marty, B., Morbidelli, A. & Pinti, D.L. (2006). Building of a habitable planet. *Earth Moon Planets* **98** (1–4), 97–151.

Martin, W. & Russell, M.J. (2007). On the origin of biochemistry at an alkaline hydrothermal vent. *Philos. Trans. R. Soc. B* **362**(1486), 1887–1925.

McCollom, T.M. & Seewald, J.S. (2003a). Experimental constraints on the hydrothermal reactivity of organic acids and acid anions: I. Formic acid and formate. *Geochim. Cosmochim. Acta* **67**(19), 3625–3644.

McCollom, T.M. & Seewald, J.S. (2003b). Experimental study of the hydrothermal reactivity of organic acids and acid anions: II. Acetic acid, acetate, and valeric acid. *Geochim. Cosmochim. Acta* **67**(19), 3645–3664.

McCollom, T.M. & Seewald, J.S. (2004). Experimental study of abiotic formation of organic compounds in hydrothermal systems. *Geochim. Cosmochim. Acta* **68**(11), A259–A259.

McCollom, T.M. & Seewald, J.S. (2007). Abiotic synthesis of organic compounds in deep-sea hydrothermal environments. *Chem. Rev.* **107**(2), 382–401.

McCollom, T.M. & Seewald, J.S. (2013). Serpentinites, hydrogen, and life. *Elements* **9**(2), 129–134.

McCollom, T.M., Seewald, J.S. & Simoneit, B.R.T. (2001). Reactivity of monocyclic aromatic compounds under hydrothermal conditions. *Geochim. Cosmochim. Acta* **65**(3), 455–468.

Moody, J.B. (1976). Serpentinization: a review. *Lithos* **9**(2), 125–138.

Nisbet, E.G. (1987). *The young Earth: An Introduction to Archaean Geology*. Cambridge University Press, Cambridge.

Nisbet, E.G. & Fowler, C.M.R. (1996). Some liked it hot. *Nature* **382**, 404–405.

Nisbet, E.G. *et al.* (1987). Uniquely fresh 2.7 Ga komatiites from the Belingwe Greenstone-Belt, Zimbabwe. *Geology* **15**(12), 1147–1150.

Normand, C., Williams-Jones, A.E., Martin, R.F. & Vali, H. (2002). Hydrothermal alteration of olivine in a flow-through autoclave: nucleation and growth of serpentine phases. *Am. Mineral.* **87**(11–12), 1699–1709.

Pizzarello, S. (2012). Catalytic syntheses of amino acids and their significance for nebular and planetary chemistry. *Meteorit. Planet. Sci.* **47**(8), 1291–1296.

Russell, M.J., Hall, A.J. & Turner, D. (1989) *In vitro* growth of iron sulphide chimneys: possible culture chambers for origin-of-life experiments. *Terra Nova* **1**, 238–241.

Russell, M.J., Daniel, R.M., Hall, A.J. & Sherringham, J.A. (1994) A hydrothermally precipitated catalytic iron sulfide membrane as a first step toward life. *J. Mol. Evol.* **39**(3), 231–243.

Russell, M.J., Hall, A.J. & Martin, W. (2010) Serpentinization as a source of energy at the origin of life. *Geobiology* **8**(5), 355–371.

Satterfield, C.N., Hanlon, R.T., Tung, S.E., Zou, Z.M. & Papaefthymiou, G.C. (1986a). Effect of water on the iron-catalyzed Fischer–Tropsch synthesis. *Ind. Eng. Chem. Prod. Res. Dev.* **25**(3), 407–414.

Satterfield, C.N., Hanlon, R.T., Tung, S.E., Zou, Z.M. & Papaefthymiou, G. C. (1986b). Initial behavior of a reduced fused-magnetite catalyst in the Fischer–Tropsch synthesis. *Ind. Eng. Chem. Prod. Res. Dev.* **25**(3), 401–407.

Schulte, M., Blake, D., Hoehler, T. & Mccollom, T. (2006). Serpentinization and its implications for life on the early Earth and Mars. *Astrobiology* **6**(2), 364–376.

Seewald, J.S., Zolotov, M.Y. & McCollom, T. (2006) Experimental investigation of single carbon compounds under hydrothermal conditions. *Geochim. Cosmochim. Acta* **70**(2), 446–460.

Seyfried, W.E. & Foustoukos, D.I. & Fu, Q. (2007). Redox evolution and mass transfer during serpentinization: an experimental and theoretical study at 200°C, 500 bar with implications for ultramafic-hosted hydrothermal systems at Mid-Ocean Ridges. *Geochim. Cosmochim. Acta* **71**(15), 3872–3886.

Sleep, N.H. (2010). The Hadean-Archaean Environment. *Cold Spring Harb Perspect. Biol.* **2**(6), a002527.

Sleep, N.H., Meibom, A., Fridriksson, T., Coleman, R.G. & Bird, D.K. (2004). H_2-rich fluids from serpentinization: geochemical and biotic implications. *Proc. Natl. Acad. Sci. USA* **101**(35), 12818–12823.

Sleep, N.H., Bird, D.K. & Pope, E.C. (2011). Serpentinite and the dawn of life. *Philos. Trans. R. Soc. B* **366**(1580), 2857–2869.

Swathi, R.S. & Sebastian, K.L. (2008). Molecular mechanism of heterogeneous catalysis. *Resonance* **13**(6), 548–560.

Valley, J.W. *et al.* (2014). Hadean age for a post-magma-ocean zircon confirmed by atom-probe tomography. *Nat. Geosci.* **7**, 219–223.

Walker, J.C.G. (1985). Carbon-dioxide on the early Earth. *Origins Life Evol. B* **16**(2), 117–127.

Wilde, S.A., Valley, J.W., Peck, W.H. & Graham, C.M. (2001). Evidence from detrital zircons for the existence of continental crust and oceans on the Earth 4.4 Gyr ago. *Nature* **409**(6817), 175–178.

Yoshida, T., Nishizawa, K., Tabata, M., Abe, H., Kodama, T., Tsuji, M. & Tamaura, Y. (1993). Methanation of CO_2 with H_2-reduced magnetite. *J. Mater. Sci.* **28**(5), 1220–1226.

Zahnle, K., Arndt, N., Cockell, C.S., Halliday, A., Nisbet, E., Selsis, F. & Sleep, N.H. (2007). Emergence of a habitable planet. *Space Sci. Rev.* **129** (1–3), 35–78.

Zahnle, K.J. (2006). Earth's earliest atmosphere. *Elements* **2**(4), 217–222.